LO-Phonon Emission Rate of Hot Electrons from an On-Demand Single-Electron Source in a GaAs/AlGaAs Heterostructure

N. Johnson,[1,2,*] C. Emary,[3] S. Ryu,[4] H.-S. Sim,[4] P. See,[1] J. D. Fletcher,[1] J. P. Griffiths,[5] G. A. C. Jones,[5] I. Farrer,[6] D. A. Ritchie,[5] M. Pepper,[2] T. J. B. M. Janssen,[1] and M. Kataoka[1,†]

[1]*National Physical Laboratory, Hampton Road, Teddington, Middlesex TW11 0LW, United Kingdom*
[2]*London Centre for Nanotechnology, and Department of Electronic and Electrical Engineering, University College London, Torrington Place, London, WC1E 7JE, United Kingdom*
[3]*Joint Quantum Centre Durham-Newcastle, School of Mathematics and Statistics, Newcastle University, Newcastle upon Tyne NE1 7RU, United Kingdom*
[4]*Department of Physics, Korea Advanced Institute of Science and Technology, Daejeon 305-701, Republic of Korea*
[5]*Cavendish Laboratory, University of Cambridge, J. J. Thomson Avenue, Cambridge CB3 0HE, United Kingdom*
[6]*Department of Electronic and Electrical Engineering, University of Sheffield, Mappin Street, Sheffield S1 3JD, United Kingdom*

(Received 30 December 2017; revised manuscript received 17 May 2018; published 26 September 2018)

Using a recent time-of-flight measurement technique with 1 ps time resolution and electron-energy spectroscopy, we develop a method to measure the longitudinal-optical-phonon emission rate of hot electrons traveling along a depleted edge of a quantum Hall bar. Comparison to a single-particle model implies the scattering mechanism involves a two-step process via an intra-Landau-level transition. We show that this can be suppressed by control of the edge potential profile, and a scattering length > 1 mm can be achieved, allowing the use of this system for scalable single-electron device applications.

DOI: 10.1103/PhysRevLett.121.137703

The development of accurate, on-demand, hot single-electron sources has opened up a new energy domain in which to study fundamental electron behavior in the solid state [1–4]. In particular, this energy domain presents a unique environment in which we can study the nature of single-particle physics and realize experiments such as electron quantum optics [5–8] and quantum technology schemes [9]. Presently, this class of experiments and technological schemes is difficult to realize because of the rapid decoherence of hot electrons, which destroy the quantum effects of interest. This inelastic scattering process is one of the reasons that high-energy quasiparticles are considered to be inappropriate for experiments that require electron coherence, such as interferometry. In order to exploit the coherence of hot electrons, we need to be able to suppress inelastic scattering modes, increasing the scattering length larger than the length scale of the electron path.

The dominant decoherence mechanism of hot electrons in GaAs systems is the energy relaxation by emission of longitudinal-optical (LO) mode phonons [10–15]. This causes the electrons to undergo a discrete energy loss ($\hbar\omega_{\mathrm{LO}} \sim 36$ meV) per emission of one LO phonon. To suppress this mode, it is important to characterize the rate of LO-phonon scattering and understand its mechanisms. However, it has so far not been straightforward to measure the rate directly in transport measurements, because, although it is relatively easy to measure the scattering probability, it is not easy to measure the electron velocity. Moreover, in the presence of a background Fermi sea, electron-electron interactions strongly affect the system, masking the simple single-particle physics [15]. Now, with the development of on-demand hot single-electron sources [1] and electron-energy spectroscopy [16], it is possible to perform an energy- and time-resolved study of hot electron transport through an intrinsic or depleted region free from electron-electron interactions.

In this work, we present measurements of the LO-phonon emission rate of hot electrons traveling in quantum Hall edge states. In order to deduce the LO-phonon emission rate, we first measure the LO-phonon emission probability P_{LO}^{l} along an electron path with length l using energy spectroscopy [16]. Then, we measure the average electron drift velocity v_d (or electron travel time $\tau = l/v_d$) in the same path using a time-of-flight measurement [17]. The scattering rate Γ_{LO} is calculated as $\Gamma_{\mathrm{LO}} = -(v_d/l)\ln(1 - P_{\mathrm{LO}}^{l})$. We perform a detailed study of how the emission rate varies as the electron energy, edge-potential profile, and magnetic field are varied. A comparison with theory for direct LO-phonon emission [18] shows that, while qualitatively in agreement, our measured rate is many orders of magnitude larger than the predicted values. We suggest that an enhanced emission process due to an inter-Landau-level transition may be present [19]. Moreover, we demonstrate that the scattering length can be made greater than 1 mm by controlling the edge potential.

A scanning-electron-microscope image of an identical device to that used, with schematic electrical connections, is shown in Fig. 1(a). The sample has a similar geometry to

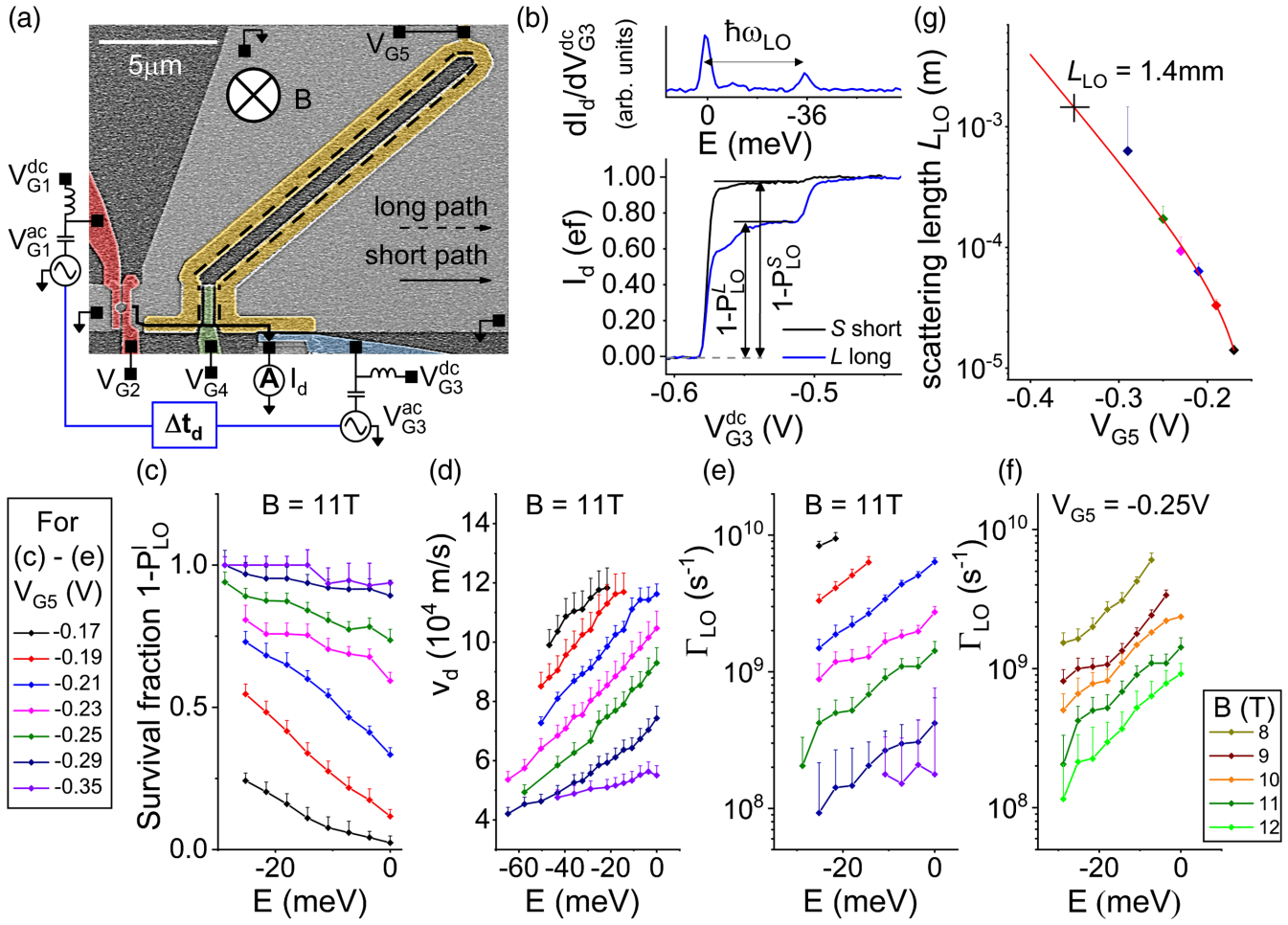

FIG. 1. (a) SEM image of the device and electrical connections. The 2DEG region is shaded in light gray. Metallic gates are colored—electron pump G_1 and G_2, red; detector gate G_3, blue; depletion gate G_5, yellow; deflection gate G_4, green. Note that the area encircled by the yellow gate, G_5, is etched away. Long and short paths are marked with dashed and solid lines, respectively. (b) Measurement of the phonon emission probability as a fraction of the pumped current, for the case of the current traveling short path S (black) and long path L (blue). The survival fraction $1-P_0^{L(S)}$ is defined as the fraction of the detector current (I_d) at the phonon plateau against ef. Above, the derivative dI_d/dV_{G3}^{dc} of the long path trace shows the energy spectrum of electrons with original emission energy (left peak) and the ones that have emitted one LO phonon (right peak), which are separated by the LO-phonon energy of 36 meV. (c)–(e) Establishing the LO-phonon emission rate at $B = 11$ T. (c) Survival fraction $1-P_{LO}^{l}$ as a function of electron emission energy E, for different values of V_{G5}. (d) Electron drift velocity v_d as a function of E, for different values of V_{G5}. (e) LO-phonon emission rate $\Gamma_{LO} = -(v_d/l)\ln(1-P_0^l)$ as a function of E, for different values of V_{G5}. (f) LO-phonon emission rate as a function of E, measured at different magnetic fields B and at $V_{G5} = -0.25$ V. (g) Scattering length $L_{LO} = v_d/\Gamma_{LO}$, for an energy $E = -25.2$ meV. A representative fit is shown in red. If we consider the strongest depletion $V_{G5} = -0.35$ V at this energy, we find $L_{LO} = 1.4$ mm (marked with a cross).

those used in Ref. [17] and is described in detail in Supplemental Material [20]. A two-dimensional electron gas (2DEG) is defined 90 nm below the surface of a GaAs/AlGaAs heterostructure. We etch the device to form the mesa shaded in light gray in Fig. 1(a) and pattern five metallic surface gates. Gates G_1 and G_2, shaded in red, define the quantum dot single-electron pump that acts as the source of energy-tunable hot electrons [1–4]. G_1 is driven by an ac sinusoidal waveform V_{G1}^{ac} at frequency $f = 400$ MHz with a peak-to-peak amplitude ~ 1 V from one channel of an arbitrary waveform generator, in addition to a dc voltage V_{G1}^{dc}. We tune the gate voltages to pump one electron per cycle, producing a current $I_p = ef \approx 64$ pA, with e the elementary charge.

In the presence of a perpendicular magnetic field B, the electrons emitted from the pump travel along the sample edge in either the short (5 μm) or long path (28 μm) indicated by the solid and dashed lines, respectively, in Fig. 1(a), just as in the edge-state transport in the quantum Hall regime [22] but with an energy (about 100 meV) above the Fermi energy E_F [16]. The voltage V_{G4} applied to the deflection gate G_4 determines which path the electrons take [20].

The time-of-flight method described in Ref. [17] gives the electron velocity in the loop section (the part that encircles the

elongated etched area and does not include the paths along gate G_4) of length $l \approx 20$ μm (see Supplemental Material [20] for a determination of this length). This is the length where we investigate the LO-phonon emission rate.

Gate G_3 (blue) is the detector gate. A dc gate voltage V_{G3}^{dc} is used to detect the electron energy [16] and the LO-phonon emission probability by measuring the transmitted detector current I_d. For the time-of-flight measurements, an ac square waveform V_{G3}^{ac}, with controllable time delay Δt_d, is applied in addition to V_{G3}^{dc} [17,23–25]. Gate G_5 (yellow) is the depletion gate and is used to change the potential profile at the edge where electrons propagate by applying a dc voltage V_{G5}. We note that, throughout this work, the voltage applied to the depletion gate is negative enough to deplete the 2DEG underneath but not negative enough to push the path of our hot electrons outside the gated region. Experiments are performed in a dilution refrigerator with a base temperature ~30 mK and with a perpendicular magnetic field of 8–12 T.

In order to determine the LO-phonon emission rate, we first measure the probability of emission in the long (short) path $P_{\mathrm{LO}}^{L(S)}$. This is done by measuring I_d while sweeping the detector V_{G3}^{dc}. This gives us a certain fraction of pumped current I_p, which is the proportion of pumped electrons that retain enough energy to pass the detector barrier. Figure 1(b) shows an example of this measurement taken for the short (black) and long (blue) paths [26]. As V_{G3}^{dc} is swept to a more positive value (i.e., as the detector barrier is lowered), I_d increases and shows a substep (the phonon plateau) before rising to ef and saturating. The derivative $dI_d/dV_{G3}^{\mathrm{dc}}$ shows two peaks as shown in the top panel in Fig. 1(b). From Ref. [16], we identify the left-hand peak as the energy spectrum of electrons at the original emission energy and the right-hand peak as that of electrons that have emitted one LO phonon before arriving at the detector. From this, we can convert the V_{G3}^{dc} scale into the energy scale, assuming $\hbar\omega_{\mathrm{LO}} \sim 36$ meV. The height of the phonon plateau (when normalized to ef) gives a survival fraction of electrons arriving at the detector without any LO-phonon emission, i.e., $1 - P_{\mathrm{LO}}^{L(S)}$ for the long (short) path.

We then deduce the survival fraction in the loop alone by noting that the long path survival fraction is the product of the survival fractions of the short path and the loop, i.e., $1 - P_{\mathrm{LO}}^{l} = (1 - P_{\mathrm{LO}}^{L})/(1 - P_{\mathrm{LO}}^{S})$. With our single-electron source, the electron emission energy can be tuned by changing the height of the exit barrier, i.e., by varying V_{G2} [16]. Figure 1(c) shows $1 - P_{\mathrm{LO}}^{l}$ as a function of the electron emission energy E (here, we define $E = 0$ for the highest emission energy used) taken with a different value of depletion gate voltage V_{G5}, at $B = 11$ T. We also measure the average electron drift velocity v_d (of the non-LO-phonon emitting fraction) in the loop section for different electron emission energies using the method described in Ref. [17] [Fig. 1(d)]. (We will later calculate the form of the edge potential profile from these data.) Assuming the constant rate of LO-phonon emission Γ_{LO} throughout the loop, we can calculate the rate as $\Gamma_{\mathrm{LO}} = -(v_d/l)\ln(1 - P_{\mathrm{LO}}^{l})$ [Fig. 1(e)] [20]. We observe that the rate of phonon emission is strongly a function of both emission energy E and V_{G5}. In Fig. 1(f), we repeat this analysis at various B values, for the case $V_{G5} = -0.25$ V. We also clearly see a strong field dependence on the rate of phonon emission, with emission suppressed at higher fields [16]. We note that the reason that there are no data below $\Gamma_{\mathrm{LO}} = 10^8$ s^{-1} in Fig. 1(e) is not because we cannot tune the device into that regime but because the scattering probability becomes so small that it is difficult to detect it by the measurement of the detector current.

We calculate the scattering length as $L_{\mathrm{LO}} = v_d/\Gamma_{\mathrm{LO}}$ and plot this in Fig. 1(g). Here, we use an example emission energy $E = -25.2$ meV, and we see clearly an increase in the scattering length with increasing V_{G5}. The red curve shows an exponential fit to these data. At this energy, and at the highest depletion gate potential $V_{G5} = -0.35$ V, we found the survival fraction $1 - P_{\mathrm{LO}}^{l} \sim 1$, and hence we could not calculate an LO-phonon emission rate. However, from the fit, we can extract an approximate scattering length, marked with the cross on Fig. 1(g), and deduce a scattering length $L_{\mathrm{LO}} = 1.4$ mm. This is an increase of several orders of magnitude with respect to $V_{G5} = 0$ and enables the realization of long coherence times for use in more sophisticated devices. The scattering length can easily be made even longer.

Because we have temporal detection of the electrons, we can detect whether the phonon emission happens uniformly around the ring, or whether there are phonon emission "hot spots." If the latter is the case, the measured phonon emission rate by our technique may not represent the actual emission rate. A phonon emission hot spot will

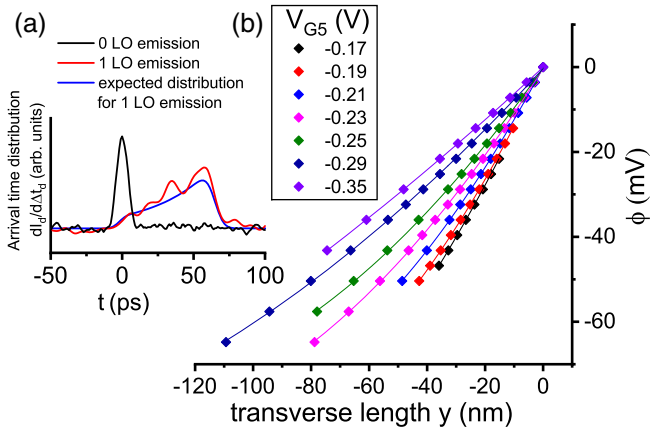

FIG. 2. (a) The arrival time distributions $A_{\mathrm{LO}}(t)$ for electrons emitting 0 (black) and 1 (red) LO phonon. The good match to the expected distribution (blue) implies that the phonon emission rate is uniform. (b) The edge potential profile ϕ, measured for different V_{G5}. We take $(y, \phi) = (0, 0)$ as the point of highest electron emission energy attainable by the pump. Solid lines show a parabolic fit, which is used to calculate the phonon emission rate.

produce a peak in the arrival-time distribution, $A_{\mathrm{LO}}(t) \propto dI_d/d\Delta t_d$, of the electrons that have emitted one LO phonon. This peak in $A_{\mathrm{LO}}(t)$ is expected to occur later than the peak of the original electrons, as the electrons at a lower energy are expected to travel at a lower velocity. However, if the phonon emission rate is constant throughout the path, we expect the arrival-time distribution to spread out as electrons emit phonons at various parts of the path. In Fig. 2(a), the measurement of arrival time distribution using the method given in Refs. [23,25] is shown for the electrons with original emission energy (black) and the electrons that have emitted one phonon (red). The expected form of $A_{\mathrm{LO}}(t)$ (blue) with a constant emission rate, as calculated from Ref. [18] (and see Supplemental Material [20]), shows a good match with the experimental data. This implies that our assumption of a constant phonon emission rate is reasonable.

Now we investigate if our experimental results can be explained within the framework of an existing single-phonon emission model [11,12,18]. To compare the measured rate against the theory, we need to know the shape of the potential profile ϕ, from which we can calculate the electronic wave function. A key parameter in the calculation of emission rates is the edge potential profile, as this dictates the spatial position of the electron before and after emission. This can be deduced from the drift velocity measurements using the method described in Ref. [17], and we plot the deduced potential profile in Fig. 2(b); for each case of V_{G5}, we have measured the LO-phonon rate, under the same conditions as the emission rate was measured.

The theoretical LO-phonon emission rate can be calculated using the method described in Ref. [18], by performing the harmonic fit to the experimentally determined potential profiles, ϕ [27]. Figure 3(a) plots the experimental data [square symbols, the same as that presented in Fig. 1(e)] and calculated LO-phonon emission rate (solid lines) for an intra-Landau-level transition ($m = 0 \rightarrow 0$, where m is the Landau level index) [red arrow in Fig. 3(b), where the horizontal axis plots the same transverse length as in Fig. 2(b)] for different values of V_{G5}. In Fig. 3(c), the ratio β of the theoretically calculated value and experimental value is plotted, showing a large discrepancy by many orders of magnitude. When only direct LO-phonon emission is considered, the predicted rates of emission are far lower than those measured experimentally. In order to explain this discrepancy, we consider the possibility that there are other paths to phonon emission.

One such possibility is a process in which an electron is first transferred to the $m = 1$ Landau level via the longitudinal acoustic via deformation potential (LADP) mode [19,28] and then is transferred back to the $m = 0$ Landau level via LO-phonon emission [see the green and blue arrows in Fig. 3(b)]. This two-step process can be faster than the direct $m = 0 \rightarrow 0$ transition. This is because the rate of any particular transition is proportional to the electronic wave function overlap and, thus, to a factor

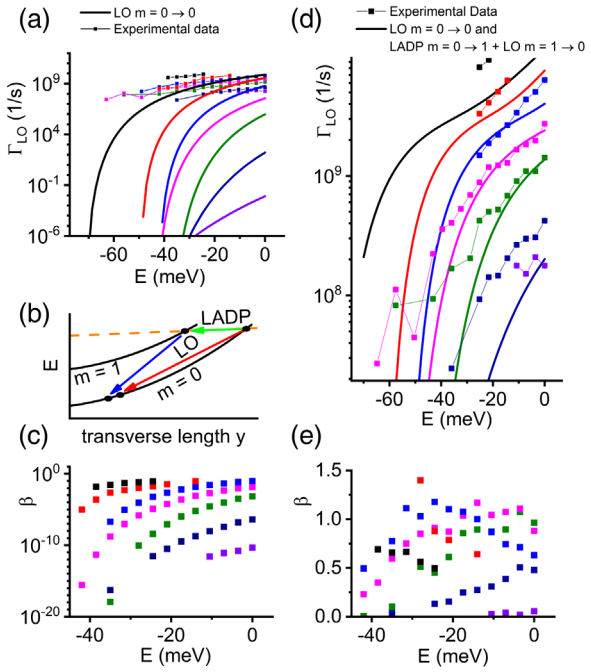

FIG. 3. (a) A comparison of measured LO-phonon emission rates [squares; colors match Fig. 1(c)] with the calculated rates for $m = 0 \rightarrow 0$ LO-phonon mode (solid lines) shows poor agreement. (b) Two lowest Landau levels at the sample edge ($m = 0$ and 1), showing the phonon scattering paths. Red arrow, $m = 0 \rightarrow 0$ LO-phonon emission; green arrow, $m = 0 \rightarrow 1$ LADP phonon emission; blue arrow, $m = 1 \rightarrow 0$ LO-phonon emission. (c) The discrepancy fraction $\beta =$ expected rate/measured rate of phonon emission for the direct ($m = 0 \rightarrow 0$) mode. (d) As in (a), with the combined rate of emission from the $m = 0 \rightarrow 0$ LO mode and the $m = 0 \rightarrow 1$ LADP emission, the $m = 1 \rightarrow 0$ LO-emission mode (solid line) shows better agreement with the data. (e) The discrepancy fraction β for the combined mode of direct and the two-step process. In this combined case, we see that we are much closer to unity.

$e^{-(\Delta y/l_b)^2/2}$, where Δy is the change in the guide-center coordinate in the transition and l_b is the magnetic length [18]. Since Δy can be smaller in each of the emissions in the two-stage process, an exponential speed-up is gained, and, in some circumstances, this can overcome the inherent slowness of a two-step process. The sum of the direct and two-step rates are shown in Fig. 3(d), and the ratio β is plotted in Fig. 3(e). This clearly shows that the calculated curves agree with experiments within an order of magnitude, except for those with the most negative values of V_{G5}. Here, the edge-confinement potential is shallower, and harmonic approximation may be inadequate, which may be the origin of the discrepancy.

In summary, we have demonstrated a detailed study of LO-phonon emission rate of hot electrons in quantum Hall edge states. We measured this rate at different electron energies and magnetic fields and under different potential profiles, which is controlled by an edge depletion gate that covers the whole electron path from the pump to the

detector. The depletion of the background electron gas allows us to study these effects within a simple single-particle picture, which had not been possible before this work, owing to the fast relaxation of the hot electron. Comparisons with the theory suggest that inter-Landau-level scattering via acoustic phonon emission is involved in the LO-phonon emission process, particularly at low energies. We found that the phonon emission rate can be controlled by the edge-depletion gate, and the scattering length can be enhanced as much as 1 mm or even longer, which enables the construction of large-scale single-electron devices using conventional nanofabrication techniques. This novel stand-alone tool can be used to realise fermionic quantum optics experiments and interferometry high above the Fermi energy. We believe this is the first such demonstration of phonon control.

We thank S. P. Giblin and S. Ludwig for useful discussions. This research was supported by the United Kingdom Department for Business, Energy, and Industrial Strategy, the United Kingdom EPSRC, and the project EMPIR 15SIB08 e-SI-Amp. This project has received funding from the European Metrology Programme for Innovation and Research (EMPIR) program cofinanced by the Participating States and from the European Union's Horizon 2020 research and innovation program and by Korea NRF (Grant No. 2016R1A5A1008184).

*Present address: NTT Basic Research Laboratories, NTT Corporation, 3-1 Morinosato Wakamiya, Atsugi, Kanagawa 243-0198, Japan.
nathan.johnson@lab.ntt.co.jp
†masaya.kataoka@npl.co.uk

[1] M. D. Blumenthal, B. Kaestner, L. Li, S. Giblin, T. J. B. M. Janssen, M. Pepper, D. Anderson, G. Jones, and D. A. Ritchie, Nat. Phys. **3**, 343 (2007).
[2] B. Kaestner, V. Kashcheyevs, G. Hein, K. Pierz, U. Siegner, and H. W. Schumacher, Appl. Phys. Lett. **92**, 192106 (2008).
[3] C. Leicht, P. Mirovsky, B. Kaestner, F. Hohls, V. Kashcheyevs, E. V. Kurganova, U. Zeitler, T. Weimann, K. Pierz, and H. W. Schumacher, Semicond. Sci. Technol. **26**, 055010 (2011).
[4] S. P. Giblin, M. Kataoka, J. D. Fletcher, P. See, T. J. B. M. Janssen, J. P. Griffiths, G. A. C. Jones, I. Farrer, and D. A. Ritchie, Nat. Commun. **3**, 930 (2012).
[5] E. Bocquillon, V. Freulon, J. M. Berroir, P. Degiovanni, B. Plaćais, A. Cavanna, Y. Jin, and G. Fève, Science **339**, 1054 (2013).
[6] E. Bocquillon, F. D. Parmentier, C. Grenier, J.-M. Berroir, P. Degiovanni, D. C. Glattli, B. Plaçais, A. Cavanna, Y. Jin, and G. Fève, Phys. Rev. Lett. **108**, 196803 (2012).
[7] M. Henny, S. Oberholzer, C. Strunk, T. Heinzel, K. Ensslin, M. Holland, and C. Schönenberger, Science **284**, 296 (1999).
[8] P. Samuelsson, E. V. Sukhorukov, and M. Büttiker, Phys. Rev. Lett. **92**, 026805 (2004).
[9] C. H. Bennett and D. P. DiVincenzo, Nature (London) **404**, 247 (2000).
[10] M. Heiblum, M. I. Nathan, D. C. Thomas, and C. M. Knoedler, Phys. Rev. Lett. **55**, 2200 (1985).
[11] S. Das Sarma and A. Madhukar, Phys. Rev. B **22**, 2823 (1980).
[12] S. Das Sarma and V. B. Campos, Phys. Rev. B **49**, 1867 (1994).
[13] U. Sivan, M. Heiblum, and C. P. Umbach, Phys. Rev. Lett. **63**, 992 (1989).
[14] D. Taubert, C. Tomaras, G. J. Schinner, H. P. Tranitz, W. Wegscheider, S. Kehrein, and S. Ludwig, Phys. Rev. B **83**, 235404 (2011).
[15] D. Taubert, G. J. Schinner, H. P. Tranitz, W. Wegscheider, C. Tomaras, S. Kehrein, and S. Ludwig, Phys. Rev. B **82**, 161416(R) (2010).
[16] J. D. Fletcher, P. See, H. Howe, M. Pepper, S. P. Giblin, J. P. Griffiths, G. A. C. Jones, I. Farrer, D. A. Ritchie, T. J. B. M. Janssen, and M. Kataoka, Phys. Rev. Lett. **111**, 216807 (2013).
[17] M. Kataoka, N. Johnson, C. Emary, P. See, J. P. Griffiths, G. A. C. Jones, I. Farrer, D. A. Ritchie, M. Pepper, and T. J. B. M. Janssen, Phys. Rev. Lett. **116**, 126803 (2016).
[18] C. Emary, A. Dyson, S. Ryu, H.-S. Sim, and M. Kataoka, Phys. Rev. B **93**, 035436 (2016).
[19] S. Komiyama, H. Hirai, M. Ohsawa, Y. Matsuda, S. Sasa, and T. Fujii, Phys. Rev. B **45**, 11085 (1992).
[20] See Supplemental Material at http://link.aps.org/supplemental/10.1103/PhysRevLett.121.137703 for more information, which includes Ref. [21].
[21] A. Fujiwara, K. Nishiguchi, and Y. Ono, Appl. Phys. Lett. **92**, 042102 (2008).
[22] B. I. Halperin, Phys. Rev. B **25**, 2185 (1982).
[23] J. Waldie, P. See, V. Kashcheyevs, J. P. Griffiths, I. Farrer, G. A. C. Jones, D. A. Ritchie, T. J. B. M. Janssen, and M. Kataoka, Phys. Rev. B **92**, 125305 (2015).
[24] N. Johnson, J. D. Fletcher, D. Humphreys, P. See, J. Griffiths, G. Jones, I. Farrer, D. Ritchie, M. Pepper, T. Janssen, and M. Kataoka, Appl. Phys. Lett. **110**, 102105 (2017).
[25] M. Kataoka, J. D. Fletcher, and N. Johnson, Phys. Status Solidi B **254**, 1600547 (2017).
[26] In this example, $V_{G2} = -0.44$ V, $V_{G5} = -0.25$ V, $B = 11$ T, and $V_{G4} = -0.3$ (short path, S) or -0.65 V (long path, L).
[27] We note that we use a z confinement (in the substrate growth direction) of 10 nm, the variation of which within 50% does not change the order of magnitude of the result and is the only free parameter in the model.
[28] J. I. Climente, A. Bertoni, G. Goldoni, and E. Molinari, Phys. Rev. B **74**, 035313 (2006).